Effects of Fe substitution on T_C suppression of MgB_2: A ^{11}B NMR study

C. S. Lue,* T. H. Su, and B. X. Xie
Department of Physics, National Cheng Kung University, Tainan 70101, Taiwan

S. K. Chen and J. L. MacManus-Driscoll
Department of Materials Science and Metallurgy, University of Cambridge, Pembroke Street, Cambridge CB2 3QZ, United Kingdom

Y. K. Kuo
Department of Physics, National Dong Hwa University, Hualien 97401, Taiwan

H. D. Yang
Department of Physics, National Sun Yat-Sen University, Kaohsiung 80424, Taiwan

(Received 15 February 2006; revised manuscript received 4 April 2006; published 6 June 2006)

We have performed a systematic study of Fe-doped MgB_2 alloys using ^{11}B nuclear magnetic resonance spectroscopy. The Knight shift, line shape, as well as spin-lattice relaxation time (T_1) on each individual composition have been identified. The central transition and quadrupole linewidths increase with Fe concentration, attributed to the effect of disorder on these measurements. The temperature independence of the central transition linewidth further confirms no magnetic moment associated with these dopants. In addition, the value of T_1T remains unchanged with Fe content, indicative of little or no effect on the B-2p Fermi level density of states (DOS) by substituting Fe in the Mg sublattice of MgB_2. These observations clearly revealed that the drop of T_C cannot be accounted for either by the pair breaking or by the electronic DOS reduction. It thus revealed the importance of the phonon contributions to the change of T_C, presumably due to the decreased phonon frequency and/or the reduced electron-phonon coupling strength through Fe doping.

DOI: 10.1103/PhysRevB.73.214505 PACS number(s): 74.70.Ad, 74.25.Nf, 74.62.Dh

I. INTRODUCTION

There is general agreement from intense experimental and theoretical research that MgB_2 is a two-gap superconductor associated with the coexistence of two-dimensional σ bands and three-dimensional π bands near the Fermi surface.[1–6] Its peculiar superconducting features have been attributed to the different electron-phonon coupling strengths in both bands. Due to the simplicity in the chemical composition, a large number of efforts have been devoted to study the chemical substitutions of MgB_2, focusing on the understanding of the nature of the parent compound as well as the possible improvement of application potential. However, only Al replacing Mg and C replacing B had been possible for higher doping level.[7] Other substitutions such as the transition metal elements in the Mg sublattice are limited to a very low concentration.[8]

Among these substitutions, the Fe-substituted MgB_2 system is of particular interest owing to the presence of Fe ions in the samples. The suppression of critical temperature (T_C) with Fe concentration is moderate (see Fig. 1)[9] as compared with single crystal $Mg_{1-x}Mn_xB_2$ where the superconductivity is lost for $x=0.02$.[10] Although the polycrystalline samples exhibit a relatively slow decrease in T_C with x,[11] presumably due to an overestimate on the Mn content arising from incomplete solubility, the magnetic pair-breaking effect has been considered as a major source for the rapid T_C drop in $Mg_{1-x}Mn_xB_2$.[10–13] In this regard, it is important to examine whether Fe ions carry magnetic moments in $Mg_{1-x}Fe_xB_2$. Together with other origins such as electronic and phonon effects, a reliable interpretation for the observed T_C variation is expected to be quite complicated. In order to clarify these effects, we performed nuclear magnetic resonance (NMR) measurement which is known as an atomic probe in metallic alloys yielding information on the intrinsic magnetism and Fermi surface features.[14] To the best of our knowledge, in spite of a significant body of work regarding the chemical substitution in the Mg sublattice of MgB_2, only the $Mg_{1-x}Al_xB_2$ system has been studied by NMR.[15–18] In this paper, we will present ^{11}B NMR results including the Knight shift, line shape, as well as spin-lattice relaxation rate for each individual composition of $Mg_{1-x}Fe_xB_2$. The information about the local environments is mainly obtained through the quadrupole interactions as well as through the hyperfine interactions in this investigation.

II. EXPERIMENT

Polycrystalline Fe-doped MgB_2 compounds were synthesized as follows. The starting precursor powders for sample preparation are crystalline magnesium (99.8%, 325 mesh) from Alfa Aesar, amorphous boron (95%–97%) from Fluka and nanoparticles of Fe_2O_3 (10–15 nm) from Pi-Kem. Nano Fe_2O_3 was used as opposed to Fe because (a) the nanoscale morphology of the Fe_2O_3 allowed for very uniform mixing, and (b) the presence of oxygen was not significant because it was already present in the Mg or B precursor. Appropriate amount of Mg and B in the stoichiometric proportion of 1:2 was first weighed and nanoparticles of Fe_2O_3 with wt. % of 0, 0.5%, 1.0%, 2.0%, and 5.0% were then added accordingly. The powders were then well mixed and ground for 60 min. This was followed by pressing the resultant powder into pellets of 5 mm in diameter and about 4 mm thick. Each of the pellets was then wrapped in Ta foil with the presence of some Mg turnings and annealed at 900 °C for 15 min with heating and cooling rate of 15 °C/min.

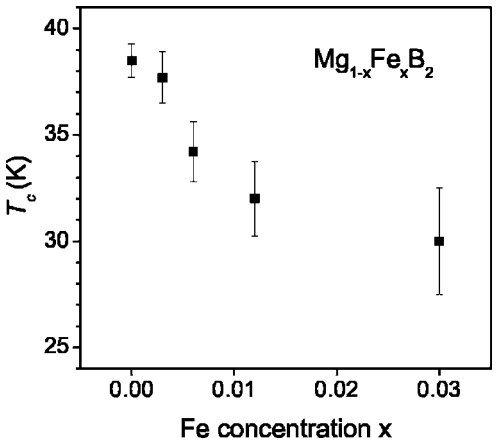

FIG. 1. Plot of critical temperature T_C as a function of Fe concentration. The error bars attached to the data points are transition width estimated from a 90% to 10% magnetization change at T_C (deduced from Ref. 9).

Room-temperature x-ray diffraction taken with Cu K_α radiation on powder specimens were consistent with the $C32$ crystal structure. Strong reflections in these alloys could be indexed according to the expected structure with several weak peaks corresponding to the MgO phase which had little effect on the NMR measurements. Based on the atomic radii of Fe (0.14 nm) and Mg (0.15 nm), it is natural to conclude that Fe atoms substitute on the Mg site rather than the B (0.085 nm) site. As illustrated in Fig. 2, lattice parameters were found to decrease linearly up to 2% Fe_2O_3 in weight, indicating that the Mg site is successfully replaced by Fe atoms, according to the Vegard's law. Therefore, it is reasonable to convert the chemical compositions to $Mg_{1-x}Fe_xB_2$ with $x=0$, 0.3%, 0.6%, 1.2%, and 3%, respectively. For $Mg_{0.97}Fe_{0.03}B_2$, however, the corresponding lattice parameters a and c deviate from the linear dependence, suggesting that this doping level is beyond the solubility limit for Fe in MgB_2. Indeed, another phase originating from FeB appears

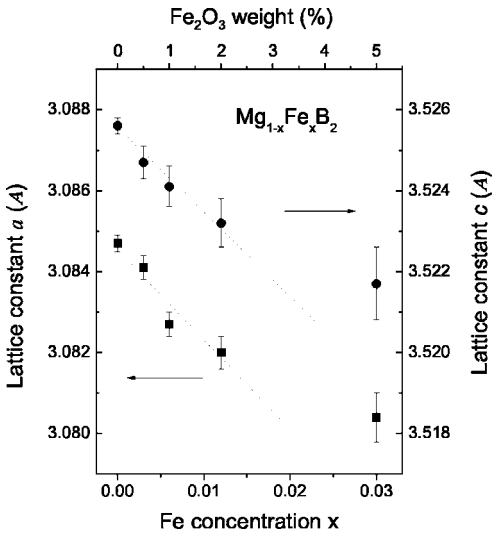

FIG. 2. Variation of lattice parameters vs Fe concentration in the series of $Mg_{1-x}Fe_xB_2$. The dotted lines indicate the linear behavior in accordance with the Vegard's law.

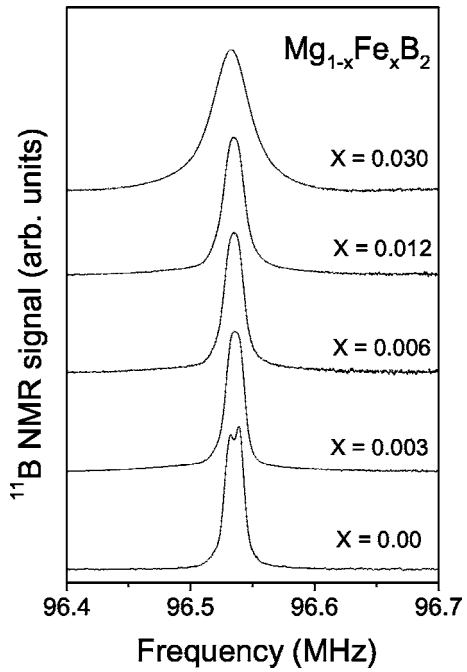

FIG. 3. Room temperature ^{11}B NMR central transition line shape for each Fe-doped MgB_2 sample.

in this material. Low Fe solubility in MgB_2 had been reported previously with the solubility limit $x \simeq 0.01$, i.e., $Mg_{0.99}Fe_{0.01}B_2$.[19,20] Although the reliable chemical formula for $Mg_{0.97}Fe_{0.03}B_2$ is unknown at this moment, for the sake of comparison, we also included the NMR results of this composition using the above index.

It is worthwhile mentioning that a considerably high solubility for $Mg_{1-x}Fe_xB_2$ has been reported up to $x \simeq 0.25$.[21] However, the corresponding T_C decrease is not as steep as that shown in Fig. 1. Since their lattice parameters do not change significantly with Fe concentration, we speculate that only partial Fe enters the crystal structure with a substantial amount of impurity phases formed in those samples. As a consequence, the Fe concentration which was taken as the nominal composition could be overestimated.

NMR experiments were performed using a Varian 300 spectrometer, with a constant field of 7.05 T. A home-built probe was employed for both room-temperature and low-temperature experiments.[22] Since the studied materials are metals, powder samples were used to avoid the skin depth problem of the rf transmission power. Each specimen was put in a plastic vial that showed no observable ^{11}B NMR signal.[23]

III. RESULTS AND DISCUSSION

Within the $C32$ crystal structure for $Mg_{1-x}Fe_xB_2$, there is a single B site with D_{3h} symmetry, leading to a symmetric one-site NMR powder pattern for each composition, as shown in Fig. 3. Here the central transition ^{11}B NMR spectra were obtained from the Fourier transform (FT) of the solid echo pulse sequence. The ^{11}B Knight shift here was determined from the position of the maximum of each spectrum with respect to an aqueous $NaBH_4$ solution reference. The

observed Knight shifts are temperature independent in the normal state, a typical character for paramagnetic metals. A small Knight shift of about 8.3×10^{-3} % ($\simeq$86 ppm) was obtained for our MgB_2, close to the values reported previously.[17,18,24] Such a tiny shift has been attributed to few *s*-character electrons at the Fermi energy, E_F.[25] The *p*-electrons also have little contribution to the Knight shift due to the low hyperfine field from *p* states, even though the B-2*p* Fermi level density of states $N_{2p}(E_F)$ is relative high in MgB_2. Note that the value of the Knight shift remains constant with the present doping level, indicative of the minor influence on $N_{2p}(E_F)$ by substituting Fe in the Mg sublattice of MgB_2.

As mentioned, the substitution of Fe in MgB_2 may produce the pair breaking effect, leading to a drop of T_C. Here the NMR linewidth could be employed to examine this magnetic effect on the resonance spectrum.[17,24] The central transition linewidth, determined from the full width at half-maximum (FWHM), is about 14 kHz for pure MgB_2. The narrow width, mainly arising from the nuclear magnetic dipolar interaction, indicates good quality of this sample. However, as shown in Fig. 4, the linewidth tends to increase with Fe concentration but still remains small values ($\simeq$35 kHz for $Mg_{0.97}Fe_{0.03}B_2$), which is not likely due to the strong local magnetism. Indeed, the linewidths were found to be temperature independent for all studied compositions, definitely proving that no magnetic moment is associated with the Fe ions.[26] Hence, the Fe impurities in MgB_2 could not act as strong magnetic scattering centers, and the possibility for the T_C suppression arising from magnetic-induced pair breaking could be excluded. Such a finding agrees well with the recently theoretical result that predicted a nonmagnetic character for Fe in MgB_2.[13]

As for the multiband superconductor MgB_2, scattering by nonmagnetic impurities should have a similar T_C suppression trend just as a pair breaking effect from magnetic impurities in conventional superconductors. For the present Fe-doping,

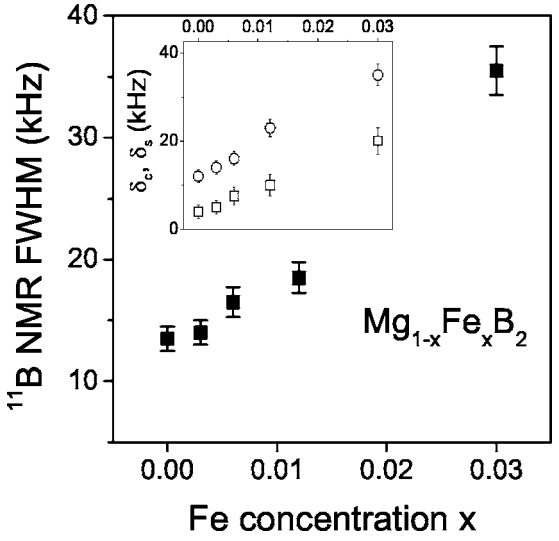

FIG. 4. Variation of ^{11}B NMR central transition linewidth as a function of Fe concentration. Broadening factors δ_c (opened squares) and δ_s (opened circles) used for the central transition and satellite lines fittings are shown in the inset.

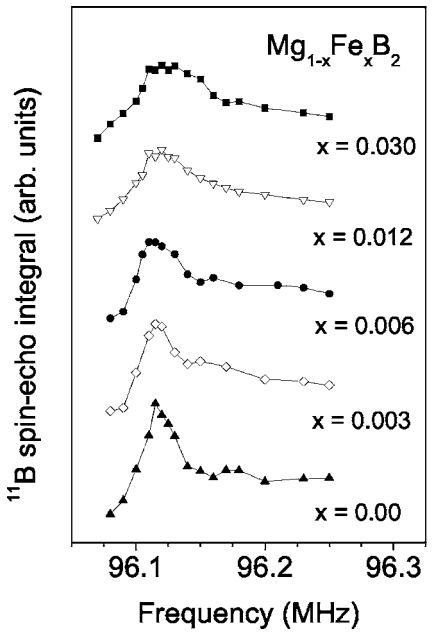

FIG. 5. Low-frequency satellite lines for the Fe-doped MgB_2 samples.

the Fe ions which are magnetically inactive would behave like nonmagnetic impurities. Accordingly, with addition of Fe in MgB_2, the degree of hyperfine field inhomogeneity enhances, resulting in a broader NMR spectrum as observed. Alternatively, such the blurred feature could be driven by distortions near the Fe sites leading to shorter B-B distances, which would result locally in an enhancement on the dipolar interaction. This effect will also introduce a modification on the local electric field gradient (EFG), leading to a change on the quadrupole frequency ν_Q. However, as we will demonstrate below, this possibility should be ruled out since no visible change in ν_Q has been found as increasing Fe concentration.

In Fig. 5, we show the low-frequency satellite line ($m=\frac{1}{2}\leftrightarrow\frac{3}{2}$ transition) for each composition, obtained from the integration of spin-echo signals. It clearly indicates that the quadrupole frequency of about 840 kHz is almost unaffected by Fe substitution, whereas the sharp satellite line edge gradually smears out as MgB_2 deviates from its stoichiometry. This observation could be accounted for by the disorder effect which introduces a distribution of the local electric field gradient and thus broaden the features of the satellite line. Such a disorder effect appears to be significant with increasing doping concentration. As a matter of fact, the observed broadening in transition width increasing with Fe content could result from the same effect.[9]

In principle, the first order quadrupole shift is the main effect shaping the satellite line, while the central line shape is affected by the second-order quadrupole interaction. Therefore, the effect of disorder should broaden both line shapes in a similar manner. To provide a convincing picture, we performed a shape function fitting with convolution to reproduce the synthetic spectra. For each individual composition, two broadening factors δ_c and δ_s were employed for the central transition and satellite line fittings, respectively. The best-simulated results (not shown here) yield the correspond-

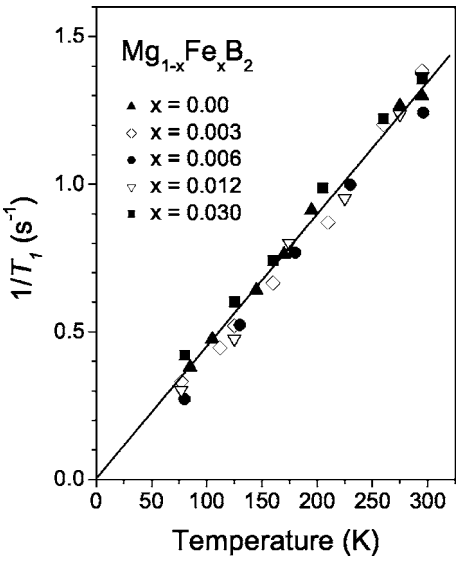

FIG. 6. Temperature dependence of ^{11}B NMR spin-lattice relaxation rate in the Fe-doped MgB_2 samples.

ing δ_c and δ_s values, which are plotted in the inset of Fig. 4 as a function of Fe concentration. As one can see, both factors correlate well with each other, indicating that the phenomena of the line broadening are essentially due to the same effect.

Band structure modifications due to disorder effect are very common in ordinary metals. Such an effect usually broadens the band width and/or shifts the Fermi energy, leading to a change of the Fermi-level density of states (DOS). In order to shed light on this scenario, we carried out the NMR spin lattice relaxation time (T_1) measurement which is known as a sensitive probe of the band structure near the Fermi level in nonmagnetic metals. We measured each T_1 by centering the resonance frequency at $m=-\frac{1}{2}\leftrightarrow+\frac{1}{2}$ transition line using the inversion recovery method. In these experiments, the relaxation process involves the adjacent pairs of spin levels, and the corresponding spin-lattice relaxation is a multiexponential expression.[27] For the central transition with $I=\frac{3}{2}$, the recovery of the nuclear magnetization follows:

$$\frac{M(t)-M(\infty)}{M(\infty)}=-2\alpha\left(\frac{1}{10}e^{-t/T_1}+\frac{9}{10}e^{-6t/T_1}\right). \qquad (1)$$

Here $M(t)$ is the magnetization at the recovery time t and $M(\infty)$ is the magnetization after long recovery time. The parameter α is a fractional value derived from the initial conditions used in our experiments. Our T_1 values were thus obtained by fitting to this multiexponential recovery curve. To provide accurate values, each T_1 has been measured several times and the averaged T_1 for each temperature was displayed in Fig. 6.

In paramagnetic metals, the spin-lattice relaxation rate measurement is a direct probe of the Fermi surface.[28] While the relaxation of nuclei in a metal is normally governed by their coupling to the spin of the *s*-character electrons, other mechanisms such as orbital and dipolar relaxation become important when the Fermi-contact term is essentially small. This would be appropriate for the case of MgB_2. From the theoretical calculations,[25] B p_σ and p_π bands are all at the Fermi level with the partial DOS $N_{p,x}(E_F)\simeq N_{p,y}(E_F)\simeq 0.035$, $N_{p,z}(E_F)\simeq 0.045$ states/eV atom. On the other hand, only a few *s* boron electrons are close to the Fermi surface [$N_s(E_F)\simeq 0.002$ states/eV atom]. The low $N_s(E_F)$ should have a minor contribution to the observed relaxation rate, in spite of the stronger hyperfine field for the B-*s* electrons at the Fermi level. This gives the dominant *p*-orbital and dipolar relaxation rates,[29] and the experimental $1/T_1T$ is mainly proportional to the square of the B-2*p* Fermi level DOS, $N_{2p}(E_F)^2$.

As indicated from Fig. 6, the T_1 results for all compositions exhibit the Korringa behavior (constant T_1T), confirming a conduction-electron mechanism for the observed relaxation. However, the value of $1/T_1T\simeq 5\times 10^{-3}$ s^{-1} K^{-1} is almost unchanged with Fe doping level, indicative of a negligible effect on $N_{2p}(E_F)$ as substituting Fe for Mg in MgB_2, being consistent with the observations in the Knight shift measurement. In these regards, the plausible T_C suppression associated with the electronic DOS reduction is unlikely based on our NMR investigations.

The absence of DOS correction with Fe content in $Mg_{1-x}Fe_xB_2$ is quite different from that in the $Mg_{1-x}Al_xB_2$ system, which shows a progressive decrease of $N_{2p}(E_F)$ with increasing the Al doping level up to $x\simeq 0.5$.[17] It is generally believed that the substitution of Al^{3+} ions in MgB_2 will dump electrons in the σ bands of the Fermi energy, leading to a reduction in the DOS.[6,30] Such a band filling effect with the corresponding changes in the DOS seems to be sufficient to understand the drop of T_C as a function of Al concentration. For the case of Fe doping, the dopants have been proposed to be trivalent ions.[13] In that case, one would expect that the nonmagnetic Fe^{3+} ions in MgB_2 will act as electron donors and have an effect similar to those of Al^{3+} ions. However, no marked change in the DOS have been found from our T_1 analysis. Such a discrepancy may be qualitatively interpreted as follows: The disorder effect causes an E_F shift to a higher DOS whereas the band filling effect reduces the DOS. As a consequence, the compensation between both mechanisms renders no visible modification in the DOS as evidenced by the present NMR measurements.

Within the BCS framework, the phonon and electronic parts play significant roles for the characteristics of T_C following the McMillian formula:[31,32]

$$T_C=\frac{\omega}{1.2}\exp\left(\frac{-1.04(1+\lambda)}{\lambda-\mu^*(1+0.62\lambda)}\right). \qquad (2)$$

Here ω, λ, and μ^* are the phonon frequency, the electron-phonon coupling constant, and a Coulomb pseudopotential, respectively. Both $\lambda=N(E_F)V_{ph}$ and $\mu^*=N(E_F)V_c$ are connected to the electronic Fermi level DOS with electron-phonon coupling constant V_{ph} and Coulomb interaction V_c. There is general agreement that the high frequency of the E_{2g} mode (ω=64–82 meV) and large λ value of about 0.7 are responsible for the unusually high T_C in MgB_2.[1,2,33] The chemical substitution is expected to alert the phonon spectrum due to either disorder or chemical pressure effects.[34] For example, Raman and infrared studies on $Mg_{1-x}Al_xB_2$

alloys have demonstrated that the Al substitution induced substantial modifications of the MgB_2 optical properties.[35] Since our NMR results clearly confirm that no electronic origin correlates to T_C via Fe doping, it thus indicates that the phonon part would be the key source for the change of T_C. We speculate that such a modification may appear in the present $Mg_{1-x}Fe_xB_2$ system. In this respect, a further investigation using optical measurements would be instructive to verify whether the frequency of the E_{2g} phonon and/or the strength of the electron-phonon coupling decrease with Fe concentration.

IV. CONCLUSIONS

We have studied the influence of Fe substitution on the T_C suppression of MgB_2 by means of the ^{11}B NMR measurement in the normal state. Results clearly revealed that the observed T_C variation cannot be accounted for either by the magnetic-induced pair breaking or by the electronic DOS reduction. We thus point to the importance of the phonon contributions to the change of T_C, presumably attributed to the decreased phonon frequency of the E_{2g} mode and/or the reduced electron-phonon coupling strength through Fe doping.

ACKNOWLEDGMENT

We are grateful for the support from National Science Council, Taiwan under Grant Nos. NSC-94–2112–M-006–001 (C.S.L.) MSC-94–2112–M-259–012 (Y.K.K.) NSC-94–2112–M-110-010 (H.D.Y.). The work in UK is supported by EPSRC.

*Electronic address: cslue@mail.ncku.edu.tw

[1] J. M. An and W. E. Pickett, Phys. Rev. Lett. **86**, 4366 (2001).
[2] J. Kortus, I. I. Mazin, K. D. Belashchenko, V. P. Antropov, and L. L. Boyer, Phys. Rev. Lett. **86**, 4656 (2001).
[3] A. Y. Liu, I. I. Mazin, and J. Kortus, Phys. Rev. Lett. **87**, 087005 (2001).
[4] H. D. Yang, J.-Y. Lin, H. H. Li, F. H. Hsu, C. J. Liu, S.-C. Li, R.-C. Yu, and C.-Q. Jin, Phys. Rev. Lett. **87**, 167003 (2001).
[5] P. C. Canfield and G. W. Crabtree, Phys. Today **56**, 34 (2003).
[6] J. Kortus, O. V. Dolgov, R. K. Kremer, and A. A. Golubov, Phys. Rev. Lett. **94**, 027002 (2005).
[7] J. Karpinski, N. D. Zhigadlo, G. Schuck, S. M. Kazakov, B. Batlogg, K. Rogacki, R. Puzniak, J. Jun, E. Muller, P. Wagli, R. Gonnelli, D. Daghero, G. A. Ummarino, and V. A. Stepanov, Phys. Rev. B **71**, 174506 (2005), and references therein.
[8] J. R. Cava, H. W. Zandbergen, and K. Inumaru, Physica C **385**, 8 (2003), and references therein.
[9] S. K. Chen and J. L. MacManus-Driscoll (private communication).
[10] K. Rogacki, B. Batlogg, J. Karpinski, N. D. Zhigadlo, G. Schuck, S. M. Kazakov, P. Wagli, R. Puzniak, A. Wisniewski, F. Carbone, A. Brinkman, and D. van der Marel, cond-mat/0510227 (unpublished).
[11] S. Xu, Y. Moritomo, K. Kato, and A. Nakimura, J. Phys. Soc. Jpn. **70**, 1889 (2001).
[12] P. P. Singh and P. Jili Thomas Joseph, J. Phys.: Condens. Matter **14**, 12441 (2002).
[13] P. Jili Thomas Joseph and P. P. Singh, cond-mat/0512675 (unpublished).
[14] C. S. Lue, B. X. Xie, S. N. Horng, and J. H. Su, Phys. Rev. B **71**, 195104 (2005).
[15] M. Pissas, G. Papavassiliou, M. Karayanni, M. Fardis, I. Maurin, I. Margiolaki, K. Prassides, and C. Christides, Phys. Rev. B **65**, 184514 (2002).
[16] H. Kotegawa, K. Ishida, Y. Kitaoka, T. Muranaka, N. Nakagawa, H. Takagiwa, and J. Akimitsu, Phys. Rev. B **66**, 064516 (2002).
[17] G. Papavassiliou, M. Pissas, M. Karayanni, M. Fardis, S. Koutandos, and K. Prassides, Phys. Rev. B **66**, 140514(R) (2002).
[18] S. Serventi, G. Allodi, C. Bucci, R. De Renzi, G. Guidi, E. Pavarini, P. Manfrinetti, and A. Palenzona, Phys. Rev. B **67**, 134518 (2003).
[19] C. H. Cheng, Y. Zhao, X. T. Zhu, J. Nowotny, C. C. Sorrell, T. Finlayson, and H. Zhang, Physica C **386**, 588 (2003).
[20] S. X. Dou, S. Soltanian, Y. Zhao, E. Getin, Z. Chen, O. Shcherbakova, and J. Horvat, Supercond. Sci. Technol. **18**, 710 (2005).
[21] Markus Kuhberger and Gerhard Gritzner, Physica C **370**, 39 (2002).
[22] C. S. Lue and B. X. Xie, Phys. Rev. B **72**, 052409 (2005).
[23] C. S. Lue and W. J. Lai, Phys. Status Solidi B **242**, 1108 (2005).
[24] S. H. Baek, B. J. Suh, E. Pavarini, F. Borsa, R. G. Barnes, S. L. Bud'ko, and P. C. Canfield, Phys. Rev. B **66**, 104510 (2002).
[25] E. Pavarini and I. I. Mazin, Phys. Rev. B **64**, 140504(R) (2001).
[26] C. S. Lue, Joseph Ross Jr., K. D. D. Rathnayaka, D. G. Naugle, S. Y. Wu, and W.-H. Li, J. Phys.: Condens. Matter **13**, 1585 (2001).
[27] W. W. Simmons, W. J. O'Sullivan, and W. A. Robinson, Phys. Rev. **127**, 1168 (1962).
[28] C. S. Lue, J. Y. Lin, and B. X. Xie, Phys. Rev. B **73**, 035125 (2006).
[29] K. D. Belashchenko, V. P. Antropov, and S. N. Rashkeev, Phys. Rev. B **64**, 132506(R) (2001).
[30] L. D. Cooley, A. J. Zambano, A. R. Moodenbaugh, R. F. Klie, Jin-Cheng Zheng, and Yimei Zhu, Phys. Rev. Lett. **95**, 267002 (2005).
[31] W. L. McMillan, Phys. Rev. **167**, 331 (1968).
[32] P. B. Allen and R. C. Dynes, Phys. Rev. B **12**, 905 (1975).
[33] S. Serventi, G. Allodi, C. Bucci, R. De Renzi, G. Guidi, E. Pavarini, P. Manfrinetti, and A. Palenzona, Phys. Rev. B **67**, 134518 (2003).
[34] K. A. Yates, G. Burnell, N. A. Stelmashenko, D.-J. Kang, H. N. Lee, B. Oh, and M. G. Blamire, Phys. Rev. B **68**, 220512(R) (2003).
[35] P. Postorino, A. Congeduti, P. Dore, A. Nucara, A. Bianconi, D. DiCastro, S. De Negri, and A. Saccone, Phys. Rev. B **65**, 020507(R) (2001).